Journal of Materials Chemistry C

Accepted Manuscript

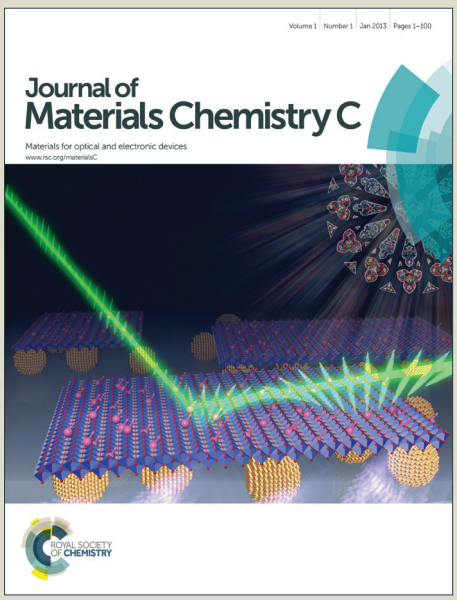

ROYAL SOCIETY OF CHEMISTRY

www.rsc.org/materialsC

Journal Name

RSCPublishing

ARTICLE

Roll to Roll Processing of Ultraconformable Conducting Polymer Nanosheets

Cite this: DOI: 10.1039/x0xx00000x

A. Zucca,[†a,b] K. Yamagishi,[†c] T. Fujie,* [c,d] S. Takeoka,[c,d] V. Mattoli* [a] and F. Greco* [a]

Received 00th January 2015,
Accepted 00th January 2015

DOI: 10.1039/x0xx00000x

www.rsc.org/

Thin and compliant conductive materials and electronic devices that are able to stand as free-standing membranes or to conform to surfaces are relevant for the development of human-device interfaces and unperceivable skin-contact personal health monitoring systems. In this work, a roll-to-roll (R2R) process for the preparation of conductive polymer nanosheets on large areas has been developed in view to move such technology towards real-world applications. R2R conductive nanosheets are obtained as free-standing structures through release from a temporary substrate and then transferred in conformal contact to any target surface with arbitrary shape, curvature and surface topography (including biological tissue such as skin). A specific high-conductivity formulation of PEDOT:PSS has been optimized for skin-contact applications, by making use of butylene glycol (BG) as dopant: a dermatologically approved ingredient. The R2R nanosheets were tested as unperceivable surface electromyography electrodes able to record muscle electric activity. The present R2R process has advantageous properties such as continuous, high throughput printing on large area rolls, cost-effectiveness, speed of execution and use of industry-ready/mass-scale manufacturing technology.

Introduction

Smart electronic skin[1], novel sensing[2], actuation and energy harvesting systems[3-5] finding application in consumer electronics, energy, robotics and biomedicine[6-8] have been made possible thanks to the improvements in the so-called field of "flexible, stretchable and conformable electronics". Such smart electronics includes thin and compliant conductive materials and electronic devices that are able to sustain bending/twisting/stretching or also to adhere and conform to surfaces.[1, 9] At the same time, industrialization of these technologies combining to the conventional film fabrication technique (e.g., R2R) is of crucial importance towards real-world applications of the smart electronics.

Technological progresses are particularly relevant for the development of human-device interfaces, implanted bio-electronics or unperceivable skin-contact personal health monitoring systems[10-13]. In this regard, a variety of conformable electronic devices that can be transferred on the skin ("epidermal electronics"[14] for thermal monitoring of the human skin[15] or epidermal hydration sensing[16, 17]) have been recently proposed, based on microfabrication of traditional inorganic materials embedded within thin elastomeric substrates.

In alternative approaches, organic conductors and semiconductors are considered because of the suitable combination of functional (mainly electronic) and structural properties. Technology related to organic and printed electronics is growing at a fast pace not only towards production of organic photovoltaics, flexible displays, OLED lighting –which constitute the major part of efforts for translating technology from lab-scale development to early production- but also towards more innovative applications, as in the case of stretchable/conformable electronics, organic bioelectronics and biointegrated technologies.[6, 12, 18-24]

Applications in cited fields, indeed, could take full advantage of the peculiar features offered by organic and printed electronics, by combining a new class of functional materials and large-area, high-volume deposition and patterning techniques.

In this framework, our group focused on the development of ultra-thin, ultra-conformable and conductive polymeric films (referred to as "conductive nanosheets") based on poly(3,4-ethylenedioxythiophene) : poly(styrenesulfonate) (PEDOT:PSS).[25] Free-standing polymer nanosheets have unique physical properties such as ultra-conformability and physical adhesiveness to biological tissues (e.g., skin, organs) due to their ultra-thin and flexible structure (tens- to hundreds-of-nanometre thickness with several square centimetres area), as in the case of PLLA nanosheets.[26-28] We previously found that the conductive nanosheets also possessed the similar structural and physical properties, that can be released in water

from their temporary substrate, manipulated as free-standing films, and recollected onto virtually any surface.[25] Moreover, various lab-scale deposition and patterning techniques permitted to embed circuits on board of nanosheets [29] and to demonstrate their utility as ultrathin actuators and sensors.[30, 31] Recently, we extended such technology to a temporary transfer conductive tattoo which was successfully employed as an unperceivable dry electrode for surface electromyography (sEMG).[32]

In view to further expand application of conductive nanosheets and to move such technology towards real-world scenarios, in this study, we focus on a roll-to-roll (R2R) process technique for the preparation of conductive polymer nanosheets with large area (several thousands of square centimetre). The present R2R process (gravure coating based) has advantageous properties such as continuous, high throughput printing on large rolls, large area patterning/processing, cost-effectiveness, speed of execution and use of industry-ready/mass-scale manufacturing technology. We choose the R2R gravure approach because of the relative simplicity and because of the availability of a small scale facility in our labs, nevertheless it should be possible to extend the methodology to other R2R techniques. The R2R conductive nanosheets can be released from a temporary substrate and obtained as free-standing, i.e. they are stable and able to support themselves without the need for any support. Then, they can be transferred in conformal contact to any target surface with arbitrary shape, curvature and surface topography (e.g. skin). The release and transfer is provided through dry peeling or wetting with water, depending on the specific formulation, with the overall transfer process being similar to that of temporary transfer tattoos. In addition, we also made use of BG, a dermatologically approved ingredient, as a secondary dopant of the conductive nanosheet for skin-contact application. The present R2R nanosheets have several advantageous characteristics, such as strength, flexibility, ability to adhere to different substrates; moreover, given the selected formulation, they could promise high biocompatibility, which could make them suitable for numerous different technological applications. In particular they could be applied in the biomedical field, as in the development of sensors and other skin-contact electronic devices and in large area flexible electronics manufacturing.

Results and discussion

R2R process and transfer of free-standing nanosheets

By using a lab-scale R2R equipment (Gravure roll coating, Fig. 1a, b) we optimized the process to fabricate: 1) single layer PEDOT:PSS nanosheets (1L) and 2) bilayer PEDOT:PSS/PDLLA nanosheets (2L). For both types of nanosheets we prepared and compared results obtained with pristine PEDOT:PSS formulation (no dopants), DMSO doped and BG doped formulations.

In summary, the R2R process (scheme in Fig. 1a) is characterized by the deposition of a polymer solution (ink) by using a roll (gravure roll) with an engraved texture that allows to print the ink on the desired flexible substrate. The gravure roll is partially immersed in the ink container and during the rotation it draws ink out of the ink container with it. A blade pushes and scrapes the roll before to contact the substrate in order to remove the excess of polymer. Then the substrate moves between the impression roll and the gravure roll; the impression roll applies a force and pushes the substrate on the gravure roll allowing the transfer of the ink. Then, a hot air flow drier included along the R2R line, provides a thermal treatment on the ink for drying it, thus obtaining a dry, homogeneous polymer film. The flexible substrate coated with film is finally collected in an output roll, by recovering it on a reel.

The 1L samples were fabricated by two steps of R2R process deposition and adopting a sacrificial layer technique in order to release the free-standing PEDOT:PSS film in acetone. During the first step a sacrificial layer of cellulose acetate has been deposited on a poly(ethylene terephthalate) (PET) film substrate; then, the layer of PEDOT: PSS was deposited on top of the sacrificial layer. The addition of 1% of fluorosurfactant Zonyl® to the pristine PEDOT:PSS water-based solution was necessary in order to improve its wetting and homogeneous spreading on the substrate. Due to the limited size of our lab-scale R2R equipment, the in-line thermal treatment provided from the drier resulted too fast and not sufficient for both drying and annealing of PEDOT:PSS. For this reason samples underwent a further off-line annealing in oven at 140 °C for 15 minutes in order to make PEDOT:PSS insoluble in water and increase its conductivity. It is important to note that, by operating the same procedure with a suitable R2R equipment – i.e. one having a properly designed length of line exposed to hot air flow (drier)- the complete thermal treatment can be operated in line in a single step with a time estimated around 60 - 180 s depending on air flow temperature, thus excluding the need for an off-line post thermal treatment. 1L nanosheets were released from the PET substrate thanks to the dissolution in acetone of the sacrificial layer of cellulose acetate.

On the other hand, the 2L nanosheets were fabricated on top of polypropylene (PP) flexible films by two steps of R2R process deposition: a first layer of PDLLA on PP substrate and a second layer of PEDOT:PSS on top of the first layer (Fig. 1c, steps i – iii, and Fig. 1 d). In this case, a PP substrate was preferred to a PET substrate because the adhesive interaction between PDLLA and PP are weaker with respect to those between PDLLA and PET and this allowed to detach the nanosheet from PP by peeling with the aid of an adhesive tape frame. This dry detachment method (Fig. 1c, steps iv – v) is particularly interesting as it does not involve the use of any solvent and permits easy manipulation of free-standing films until their transfer on target surfaces. The adhesive tape was placed on top of the 2L nanosheet still supported on PP; then, with the aid of tweezers, the bilayer was detached from the substrate obtaining a freestanding membrane supported by an adhesive tape frame (steps iv-v, Fig. 1c and Fig. 1e). The nanosheet was then temporarily transferred onto a piece of nylon mesh (step vi) that allows the subsequent detachment and transfer of the nanosheet

on the skin by wetting its surface with water, in a similar fashion of a temporary transfer tattoo (steps vii-ix, Fig. 1c). In the case of 1L nanosheets, they can be recollected on the same mesh from release baths where they float free-standing (Fig. 1 e) and then transferred according to the same vi-ix steps. A video showing the sequence of peeling, transfer and release on skin is available as Supporting Information (SI1).

Due to their ultra-low thickness and composition, nanosheets are characterized by stable and conformal adhesion to a variety of different surfaces -such as tissues or soft and rigid materials with complex topography and non-planar shapes- while maintaining their conductive functionality. These features are very important for the envisioned applications in the field of skin-contact electronics. Some examples of very large area nanosheets transferred on human skin are provided in Fig. 1f.

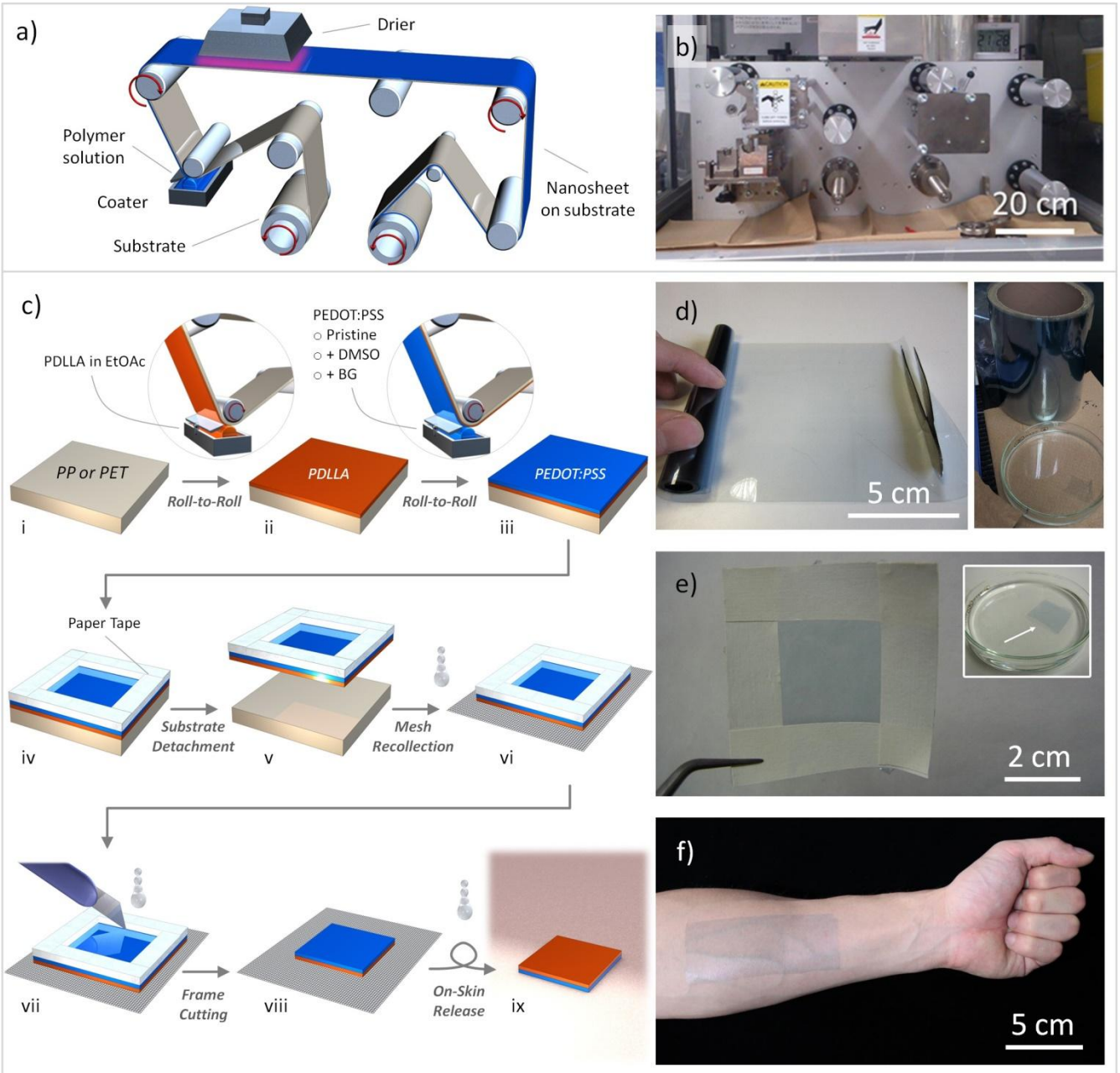

Fig. 1 Schematic view of R2R gravure roll coating technique (a) and picture of the lab-scale R2R equipment. Scheme of processing, release and transfer steps for 1L and 2L conductive nanosheets (c). d) Pictures of PP rolls on which 2L conductive nanosheets have been fabricated. e) Free-standing nanosheet peeled off from temporary substrate by means of an adhesive tape frame. f) Example of conductive nanosheet transferred on skin.

Structural and electrical characterization

Thickness of nanosheets could be controlled by setting R2R process parameters. In the case of 1L nanosheets thickness was

varied in the range 60 - 150 nm by changing the gravure roll rotation speed used in the R2R deposition (Fig. 2a). Similar results were obtained for all of three PEDOT:PSS compositions taken in consideration –i.e. pristine (no dopants), DMSO doped and BG doped- with a linearly increasing thickness with increasing gravure roll speed. As regards 2L nanosheets, PEDOT:PSS layer deposition was set to 25 rpm gravure roll speed, and overall thickness was varied by varying the PDLLA concentration in the solution used for gravure roll coating (Fig. 2b). The thickness of single layer PDLLA nanosheet is reported for a purpose of useful comparison. Overall thickness of 2L nanosheets was in the range 180 - 380 nm, which included a PDLLA layer with thickness in the range of 70-170 nm. Thickness of PDLLA layer was found to linearly increase as PDLLA concentration was increased from 1 - 2 wt.%.

Conductivity σ of nanosheets was investigated by using a 4-point probe measurement system on square samples. Addition to PEDOT:PSS of secondary dopants such as ethylene glycol, dimethyl sulfoxide, sorbitol or others in a typical range of 1−10 wt. % content is known to greatly enhance the electronic conductivity of dried films.[33-35] To this aim, we added a 5 wt. % of DMSO or BG to the original PEDOT:PSS formulation. BG was especially selected for skin-contact applications of conductive nanosheets since it is normally used as an additive in several cosmetic products to be applied on skin, and thus promises possible biocompatibility.[36] A comparison of the conductivity σ of the 1L nanosheets made with pristine PEDOT:PSS and doped PEDOT:PSS is reported in Fig. 2c.

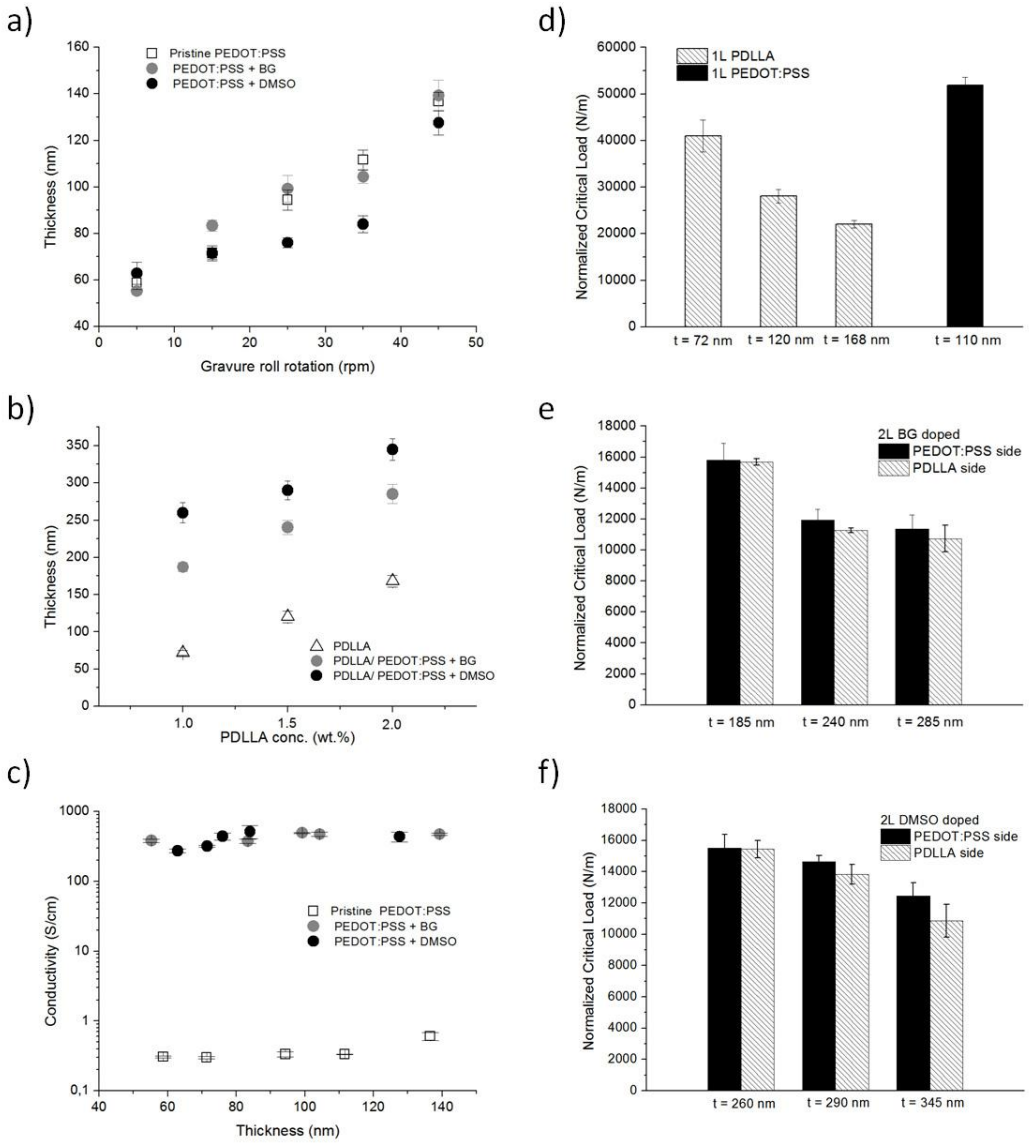

Fig. 2 a) Thickness of 1L nanosheets as a function of gravure roll speed in R2R process; b) thickness of 2L nanosheets as a function of PDLLA concentration in R2R process; c) conductivity of nanosheets as a function of thickness; comparison among different formulations of the conductive layer: PEDOT:PSS (open squares), PEDOT:PSS+BG (grey circles), PEDOT:PSS+DMSO (black circles). Evaluation of adhesive strength of nanosheets on Si surface with a scratch tester: Normalized Critical

Load for d) 1L nanosheets, comparison among PDLLA (various thickness depending on PDLLA concentration) and PEDOT:PSS; 2L nanosheets with BG e) and DMSO f) as doping agents in PEDOT:PSS, comparison among nanosheets at different thickness for PDLLA and PEDOT:PSS side.

The doping effect of both DMSO and BG is clearly demonstrated with typical conductivity enhanced by three order of magnitude with respect to pristine PEDOT:PSS. This conductivity enhancement is totally in line with expectations and values reported in literature for PEDOT:PSS films containing similar dopants and deposited on bulk substrates.[34, 37] Conductivity of the ultra-thin PEDOT:PSS nanosheets slightly increased by increasing thickness, as already observed for nanosheets with similar thickness range. This evidence was rationalized by considering the onset of some percolation effect arising at low thickness, comparable with typical dimension of primary PEDOT-rich particles.[25, 38]

Adhesive strength

Further characterization of R2R nanosheets involved the assessment of their adhesive properties. Indeed, once nanosheets are recollected on target surfaces –onto which they conform because of ultra-low-thickness- they are characterized by stable adhesion and interfacing, mainly due to Van Der Waals interaction between surface and nanosheets. The adhesion properties of the nanosheets has been evaluated by investigating the relationship between the critical load necessary for their detachment from the substrate and their thickness, by using a scratch tester for thin films.[39]

A diamond tip gradually scratched the nanosheet collected onto a Si wafer causing the detachment from the substrate thereafter measured from obtained images. We evaluated the adhesion properties both of 1L and 2L nanosheets. In the latter case, each side of the PEDOT:PSS/PDLLA bilayer nanosheet (with pristine PEDOT:PSS formulation) was tested.

As a general trend, the adhesion strength increased as thickness decreased both for 1L and for 2L nanosheets (Fig. 2d, e, f). This trend is consistent with the adhesive properties of other single layer nanosheets such as poly(L- lactic acid) (PLLA) and poly(lactic-co-glycolic acid) (PLGA).[40, 41] For free-standing nanosheets with thickness less than 100 nm, we observed higher potential to adhere to several substrates without any kind of reagents or surface functionalization. This adhesion property strongly decreased as thickness increased. Indeed as concerns PDLLA nanosheets (Fig. 2d), the critical load varied from ~ 40000 N/m for a thickness of ~ 70 nm to ~ 22000 N/m for a thickness around 170 nm. Instead, the 1L PEDOT:PSS nanosheet (thickness ~ 110 nm) showed higher critical load compared with PDLLA nanosheets (Fig. 2d).

Regarding the 2L nanosheets, by comparing the results obtained between the opposite sides of the nanosheets, a higher critical load was found for the PEDOT:PSS side rather than the PDLLA side, for both BG (Fig. 2e) and DMSO (Fig. 2f) doped PEDOT:PSS, respectively. The difference in normalized critical load between PEDOT:PSS surface and PDLLA surface slightly increased by increasing the thickness of PDLLA layer, while no significant variations of adhesion trends were observed for different formulations of PEDOT:PSS. It is suggested that difference in the adhesion properties would be attributed to the mechanical properties of each nanosheet surface. Considering that adhesive strength of nanosheets increases as elastic modulus decreases,[27] PEDOT:PSS nanosheets (< 1 GPa) may show higher adhesive strength than the PDLLA nanosheets (~3 GPa)[25, 42].

Stability of nanosheets on skin: mechanical stress and sweat

Because one of the envisioned applications of R2R conductive nanosheets is as skin-contact unperceivable electrodes, we studied how their electric properties are affected when collected on human skin. A first source of variation and/or damage to the integrity of nanosheets and to their functional behaviour could come from mechanical stress, in particular during exercising. Particularly severe conditions apply when the target area for placement of the nanosheet electrode is on rather stretchable/movable parts of the body; in such cases a wearable device can be subjected to relatively high levels of stretching/bending/compression. To this purpose, we assessed the stability and evolution of electrical resistance of nanosheets placed on the wrist and on the finger, contacted with Au coated polyimide thin sheet electrode and subjected to repetitive cycles of flexion/exercise. These target body parts are indeed selected as most representative of severe mechanical constraints. Results of the experiments are summarized in Fig. 3a. It is interesting to notice that when subjected to repeated stimulation up to 250 cycles, only negligible irreversible variations of electrical resistance were observed in the case of wrist (expansion/contraction on a +42/-42° range with respect to relaxed state – 0°) and minor variations (up to 20%) in the case of finger contraction, where nanosheet was placed across distal phalanges (flexion 70°). Such a variation of electrical resistance can be ascribed to the formation of cracks that partially interrupt the structural integrity of the nanosheet.

Moreover, by visually inspecting the nanosheet surface and the nanosheet/electrode interface after cyclic exercising we were able to recognize that cracks are mostly formed at the nanosheet/electrode interface: indeed interfacing of the ultrathin nanosheet with a considerably thicker (13 μm) and stiffer Au/polyimide electrode can cause ruptures along the edge. Furthermore, visual inspection of nanosheet worn on the skin of subjects for a longer period and during exercising (a football match) did not evidenced the formation of cracks (Fig. 3b).

Thus it is expected that even better performances in term of resistance stability to mechanical stress can be obtained if suitable solutions for contacting are addressed. A second source of variation/degradation of electrical performances for electrodes worn on skin could come from sweating. In order to assess the nanosheet stability against sweating nanosheets were immersed in a bath containing water or artificial sweat at two different pH levels (namely pH 5.5 – often referred to as "physiological skin pH"- and pH 8, representative of basic conditions encountered, for example, during aging or in

presence of some pathologies[43]), and their electrical resistance was monitored over time up to 3 h of immersion. While structural integrity was preserved (Fig. 3 c i), an increase in electrical resistance was observed in all cases (Fig. 3c, iii), with lower variation recorded for immersion in water (R/R_0 ~ 2 after 3 h). Physiological condition (pH 5.5) caused a variation of R/R_0 ~ 3 after 3 h, while basic conditions (pH 8) were more aggressive, with a distinct variation R/R_0 ~ 7-8 after 3 h. Reduced stability of the conductive properties of PEDOT:PSS in a basic environment have been reported previously, and ascribed to oxidative processes[44] or to the decrease of the carrier density and the carrier mobility due to alkaline components (such as NaOH).[45] Nevertheless, despite the harsh condition of experiments, which are worse than real sweating condition on skin, the nanosheets demonstrated to fully retain their structural integrity and at least partially retain their functional properties. In order to compare the stability against sweating of nanosheets with that of other skin-contact electrodes, a standard pregelled sEMG electrode was immersed in a bath containing artificial sweat at pH 8.0 for 3 h. The pregelled electrode was irreversibly damaged as clearly evidenced in pictures (Figure 3 c ii).

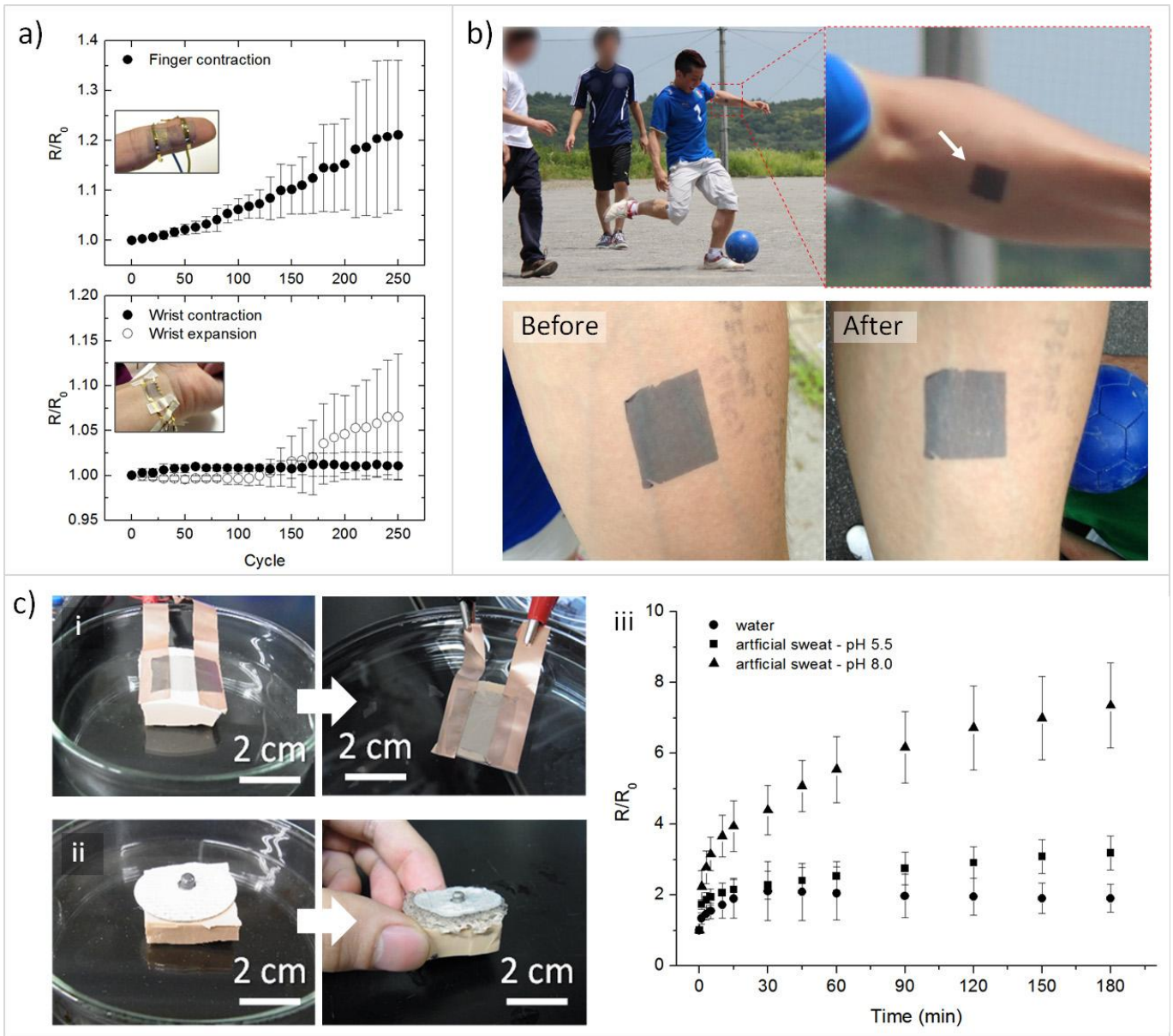

Fig. 3 Evaluation of function/stability on skin of BG doped 2L nanosheets. a) Stability against mechanical stress: electrical resistance variation R/R_0 during repeated exercise for finger contraction (nanosheet placed on distal phalanges, flexion 70° respect to relaxed state) and wrist contraction/expansion (nanosheet placed on wrist, flexion +42/-42° respectively respect to relaxed state). b) Evaluation of nanosheet integrity for a nanosheet worn on the skin of a subject during exercise (football match). c) Stability against sweating: pictures of samples before (left) and after (right) immersion for 3 h in artificial sweat (pH 8.0) in the case of 2L nanosheet (i) and standard pregelled sEMG electrode (ii); (iii) evolution during time of electrical resistance variation R/R_0 of nanosheets collected on a silicone replica of skin and submerged in a bath containing water (squares), artificial sweat - pH 5.5 (squares) and pH 8.0 (triangles).

Operation of nanosheets as sEMG electrodes

As a preliminary demonstration of applications of the present nanosheets as on-skin electrodes for personal healthcare monitoring, we tested their performances as dry surface electromyography (sEMG) electrodes. By using a standard EMG setup connected to conductive nanosheets adhered on skin through thin Au coated plastic foils, we were able to record the electric activity of muscles on the arm of one healthy subject. Experiments were performed in parallel also with standard pregelled Ag/AgCl sEMG electrodes used in clinical practice, to provide a meaningful comparison. Stepwise increment of the sEMG signals were recorded as a function of the pressure applied by a hand grasping an analogue pressure gauge (Fig. 4a), while no sEMG signals were recorded after removal of the nanosheets (Fig. 4b). Notably, comparable results were obtained, especially in terms of signal to noise ratio (SNR). Such promising results are totally in line with those recently obtained in the case of PEDOT:PSS temporary transfer tattoos.[32] The demonstrated capability of nanosheets to act as dry sEMG electrodes could open the way toward healthcare monitoring application as well as to fascinating fields of use of EMG as in the case of prosthetic limbs.[46, 47]

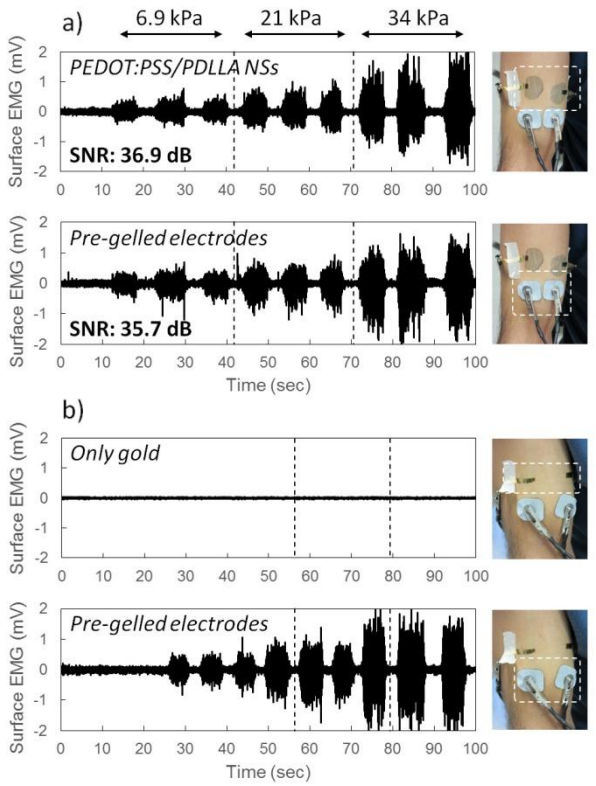

Fig. 4 sEMG recording of muscle activity (contraction) on the arm of a healthy subject: a) comparison between 2L BG-doped nanosheets and standard pregelled electrodes, and b) comparison between no nanosheets and pregelled electrodes. Signal to noise ratio (SNR) of a recorded signal demonstrating similar performances.

Conclusions

A method was presented for the fabrication of single layer (1L) and bilayer (2L) conductive nanosheets with a R2R process, characterized by high throughput and capability to operate on very large area. Nanosheets can be obtained as free-standing membranes after release from a temporary substrate with a wet (sacrificial layer) or dry (mechanical peeling off) methods, and used as ultra-thin ultraconformable electrodes. Three different formulations of the conducting polymer layer were optimized and tested for achieving different grades of conductivity and to address the requirements of specific applications. In particular an high conductivity grade formulation was demonstrated making use of a dermatologically safe doping agent (BG), to be used for skin-contact applications of the present nanosheets.
Nanosheets were characterized as regards their structure and their functional properties also on skin and a first proof of principle demonstration of operation as dry sEMG electrodes was presented.
These findings could open the way to the development of free-standing ultrathin conductive membranes and of unperceivable and low-cost on-skin electrodes for applications in sports, wellness and healthcare.

Experimental

Materials.

Rolls of poly(propylene) (PP) (TORAYFAN® 2500H) with a thickness of 40 μm and poly(ethylene-terephtalate) (PET) (Lumirror® T60) with a thickness of 25 μm were purchased from Toray and were used as received as substrates for nanosheet preparation. A PEDOT:PSS aqueous dispersion, Clevios PH1000 (1:2.5 PEDOT:PSS ratio; H.C. Starck GmbH, Leverkusen, Germany) has been employed after filtration (MILLEX average pore size 0.8 μm, MILLIPORE). Poly (D,L-lactic acid) (PDLLA, M_w = 330- 600 kDa) was purchased from Polysciences Inc. and used as received. Cellulose acetate (CA, average M_w = 30 kDa) was purchased from Sigma-Aldrich and used as received. Ethyl acetate (≥99.5%, Wako Pure Chemical Industries, Ltd), dimethyl sulfoxide (DMSO, Wako Pure Chemical Industries, ≥99%), acetone (≥99%, Wako Pure Chemical Industries), Zonyl® FS- 300 Fluorosurfactant (laboratory grade, Sigma- Aldrich) were used without any other purification.

Fabrication of Single Layer PEDOT:PSS R2R Nanosheets.

PEDOT:PSS nanosheets were prepared by using a sacrificial layer technique, by properly modifying the process reported elsewhere. CA (c = 20 mg/ml in acetone) was used as the sacrificial layer and it was deposited on a PET film substrate by a roll to roll (R2R) process technique at 30 rpm (gravure roll rotation) with a line speed of 1.3 m/min and then dried at 80 °C, with an hot air flow included in the R2R line. The PET film coated with CA was obtained in a roll, after recovery by winding on a reel. The PEDOT:PSS acqueous dispersion (Clevios PH 1000) was mixed with DMSO (5 wt. %) or with BG (5 wt.%) and Zonyl FS- 300 (1 v/V %) for 8 h at RT with

the aid of a magnetic stirrer and then deposited using a R2R process technique over the dried CA layer. The gravure roll rotation was varied in the range between 5 rpm and 45 rpm for obtaining nanosheets with different thicknesses, while line speed was kept constant at 0.2 m/min. Then samples underwent a short thermal treatment at 130 °C with an hot air flow integrated in the R2R line and re-reeled. A subsequent thermal treatment in oven at 140 °C for 15 minutes was imposed to the roll. PEDOT:PSS nanosheets were finally released in acetone after the dissolution of CA layer.

Fabrication of Bilayer PEDOT:PSS/PDLLA R2R Nanosheets.

PEDOT:PSS/PDLLA bilayer nanosheets were prepared by using a R2R process technique. PDLLA (*c* = 1- 1.5- 2 wt. % in ethyl acetate) was deposited onto a PP film substrate at 25 rpm, a line speed of 1.3 m/min and then dried at 80 °C with an air flow in R2R line. The PP film coated with PDLLA was obtained in a roll, after recovery by winding on a reel. The PEDOT: PSS acqueous dispersion (Clevios PH 1000) was mixed with DMSO (5 wt. %) or with BG (5 wt.%) and Zonyl (1 V/ v %) for 8 h at RT with the aid of a magnetic stirrer and deposited using a R2R process technique over the cured PDLLA layer at 35 rpm (gravure roll rotation) with a line speed of 0.2 m/min and then dried with an air flow in R2R line at 130 °C. A post thermal treatment in oven at 110 °C was carried out on the re-reeled roll. The bilayers of PEDOT: PSS/ PDLLA were peeled from the PP substrate by using tape attached on the edges of the nanosheet.

Thickness, Surface and Electrical Characterization.

Thickness of the conductive polymer nanosheets was obtained by Atomic Force Microscope (AFM) imaging, operating in tapping mode (MFP-3D-BIO, Asylum Research Co., Santa Barbara, CA). Measurements were performed in air, at room temperature, on samples collected and dried on a fresh silicon wafer after the release of the nanosheet. The thickness t was measured by scratching the nanosheet with a needle. From AFM topographic imaging between the nanosheet and the scratched domain (scan range area 20 x20 μm^2) it was possible to quantify the thickness of the nanosheet, by measuring the height profile of the edge.

The electrical characterization of the nanosheets was carried out with a four-point technique on square samples with lateral dimension of 1.5 cm. Sheet resistance *Rs* was measured and the related conductivity σ has been calculated making use of formulae: $Rs = \pi/ln2\ (V/i)$; $\sigma = 1/\ Rs\ t$.

Adhesive Properties Characterization of the Nanosheets.

The adhesion strength of the conductive nanosheets was measured by a scratch tester for thin films (model CSR-02, Rhesca, Tokyo) with the following procedure: a diamond tip with a radius of curvature of 100 μm was continuously and vertically loaded at a rate of 10 mN/min, and used to horizontally scratch the conductive nanosheet readsorbed on the SiO_2 substrate (scratch length: 100 μm, scratch rate: 10 mm/s). The signal of frictional vibration just after breaking of the nanosheet was detected (designated a critical load). The critical loads were measured on nanosheets collected onto fresh silicon wafer and the measures were performed on single layer PEDOT:PSS, PDLLA single layer nanosheets and PDLLA/PEDOT:PSS bilayer nanosheets by changing thickness of the PDLLA layer. Critical loads were normalized by dividing the obtained values by the nanosheet thickness.

Evaluation of stability of the nanosheets as skin-contact electrodes.

Experiments were performed on 2L nanosheets with PEDOT:PSS including BG as a dopant. Stability and evolution of electrical resistance of nanosheets subjected to repetitive cycles of flexion/exercise on skin was assessed by placing square samples on the wrist and on the finger of one subject. Electric contact with nanosheets was provided by two Au coated polyimide thin sheet (thickness 13 μm) placed at opposite edges of nanosheet. The resistance across electrode and nanosheet was recorded with a digital multimeter during exercising (flexion) of wrist and distal phalanges of finger. Stability of nanosheets against sweating was assessed by prolonged (up to 3 h) immersion of nanosheet samples in water and artificial sweat (JIS L0848, Isekyu) at pH 5.5 and pH 8.0. The 2L nanosheets were adhered to an artificial skin model (Product No. 47, Inner arm model from woman, Beaulax) with PEDOT:PSS side bottom. Electrical contact between a nanosheet and a digital multimeter was provided with two pieces of conductive copper tape sealed on the skin model. The skin model with adhered nanosheet was immersed in MilliQ water, acidic (pH 5.5) artificial sweat solution, or alkaline (pH 8.0) artificial sweat solution and the resistance across the nanosheet was recorded at the period of 1, 3, 5, 10, 15, 30, 45, 60, 90, 120, 150, and 180 min after immersion. Measurements were taken on three different samples for each.

sEMG experiments.

2L nanosheets with PEDOT:PSS including BG as a dopant were tested as dry sEMG electrodes. Circular samples (diameter 2 cm) were placed on top of the upper arm of a healthy subject. Standard pregelled Ag/AgCl sEMG disposable electrodes (gel area diameter 2 cm; Eurotrode) were placed in parallel to the nanosheets for comparison. The subject was asked to grasp an analog pressure gauge in hand. (North Coast Medical, Morgan Hill, CA) and to maintain the grip force at three levels (1, 3, 5 pounds/in.^{2}, psi) as indicated by the gauge, while the EMG was being recorded. The contraction and relaxation of the muscle were repeated alternately for three times for each pressure level. The sEMG signals were acquired by using a versatile amplifier (EMG-USB2$^+$, OT Bioelettronica) and the original data were analyzed by Excel 2013, Microsoft. The SNR was calculated by taking the highest EMG signal peak (A_s) during active period and the standard deviation (STD) of the background (A_n) during inactive period. From these values, the *SNR* was calculated by the following formula:

$$SNR\ (\mathrm{dB}) = 20 \log_{10} \frac{A_s}{A_n}.$$

Acknowledgements

The help of Dr. Sudha (Istituto Italiano di Tecnologia) for providing suitable means of contacting nanosheets on skin is acknowledged. Dr. Christian Cipriani and Mr. Sergio Tarantino (The Biorobotics Institute, Scuola Superiore Sant'Anna, Pisa, Italy) are acknowledged for their help in sEMG experiments. This work was supported in part by JSPS Core-to-Core Program (K.Y., T.F. and S.T.) from MEXT, Japan, Institute of Advanced Active Aging Research, Waseda University (K.Y., T.F. and S.T.), the Leading Graduate Program in Science and Engineering, Waseda University from MEXT, Japan (K. Y.), and Mitsubishi Materials Research Grant (T.F.).

Notes and references

[a] Center for Micro-BioRobotics@SSSA, Istituto Italiano di Tecnologia, Viale R. Piaggio 34, 56025, Pontedera, Italy. Email: virgilio.mattoli@iit.it, francesco.greco@iit.it
[b] The Biorobotics Institute, Scuola Superiore Sant'Anna, Viale R. Piaggio 34, 56025, Pontedera, Italy.
[c] Graduate School of Advanced Science and Engineering, Waseda University, TWIns, 2-2 Wakamatsu-cho, Shinjuku, Tokyo 162-8480, Japan. Email: t.fujie@aoni.waseda.jp.
[d] Institute of Advanced Active Aging Research, Waseda University, TWIns, 2-2 Wakamatsu-cho, Shinjuku, Tokyo 162-8480, Japan.

† These authors equally contributed to work

Electronic Supplementary Information (ESI) available:

Supporting Video 1 shows a demonstration of peeling off, handling and release on skin of a 2L conductive nanosheet.

See DOI: 10.1039/b000000x/

1. S. Bauer, *Nat Mater*, 2013, **12**, 871-872.
2. H. Tao, M. A. Brenckle, M. Yang, J. Zhang, M. Liu, S. M. Siebert, R. D. Averitt, M. S. Mannoor, M. C. McAlpine, J. A. Rogers, D. L. Kaplan and F. G. Omenetto, *Advanced Materials*, 2012, **24**, 1067-1072.
3. R. D. Kornbluh, R. Pelrine, H. Prahlad, A. Wong-Foy, B. McCoy, S. Kim, J. Eckerle and T. Low, *MRS Bulletin*, 2012, **37**, 246-253.
4. W. Jia, G. Valdés-Ramírez, A. J. Bandodkar, J. R. Windmiller and J. Wang, *Angewandte Chemie*, 2013, **125**, 7374-7377.
5. S. Bauer, S. Bauer-Gogonea, I. Graz, M. Kaltenbrunner, C. Keplinger and R. Schwödiauer, *Advanced Materials*, 2014, **26**, 149-162.
6. T. Someya, *Stretchable Electronics*, 2012.
7. D.-H. Kim, J. Xiao, J. Song, Y. Huang and J. A. Rogers, *Advanced Materials*, 2010, **22**, 2108-2124.
8. T. Someya, Y. Kato, T. Sekitani, S. Iba, Y. Noguchi, Y. Murase, H. Kawaguchi and T. Sakurai, *Proceedings of the National Academy of Sciences of the United States of America*, 2005, **102**, 12321-12325.
9. M. L. Hammock, A. Chortos, B. C. K. Tee, J. B. H. Tok and Z. Bao, *Advanced Materials*, 2013, **25**, 5997-6038.
10. J. Viventi, D.-H. Kim, L. Vigeland, E. S. Frechette, J. A. Blanco, Y.-S. Kim, A. E. Avrin, V. R. Tiruvadi, S.-W. Hwang, A. C. Vanleer, D. F. Wulsin, K. Davis, C. E. Gelber, L. Palmer, J. Van der Spiegel, J. Wu, J. Xiao, Y. Huang, D. Contreras, J. A. Rogers and B. Litt, *Nat Neurosci*, 2011, **14**, 1599-1605.
11. D.-H. Kim, J. Viventi, J. J. Amsden, J. Xiao, L. Vigeland, Y.-S. Kim, J. A. Blanco, B. Panilaitis, E. S. Frechette, D. Contreras, D. L. Kaplan, F. G. Omenetto, Y. Huang, K.-C. Hwang, M. R. Zakin, B. Litt and J. A. Rogers, *Nature Materials*, 2010, **9**, 511-517.
12. D. Khodagholy, T. Doublet, M. Gurfinkel, P. Quilichini, E. Ismailova, P. Leleux, T. Herve, S. Sanaur, C. Bernard and G. G. Malliaras, *Advanced Materials*, 2011, **23**, H268-H272.
13. P. Leleux, J.-M. Badier, J. Rivnay, C. Bénar, T. Hervé, P. Chauvel and G. G. Malliaras, *Advanced Healthcare Materials*, 2013, n/a-n/a.
14. D. H. Kim, N. Lu, R. Ma, Y. S. Kim, R. H. Kim, S. Wang, J. Wu, S. M. Won, H. Tao, A. Islam, K. J. Yu, T. I. Kim, R. Chowdhury, M. Ying, L. Xu, M. Li, H. J. Chung, H. Keum, M. McCormick, P. Liu, Y. W. Zhang, F. G. Omenetto, Y. Huang, T. Coleman and J. A. Rogers, *Science*, 2011, **333**, 838-843.
15. R. C. Webb, A. P. Bonifas, A. Behnaz, Y. Zhang, K. J. Yu, H. Cheng, M. Shi, Z. Bian, Z. Liu, Y.-S. Kim, W.-H. Yeo, J. S. Park, J. Song, Y. Li, Y. Huang, A. M. Gorbach and J. A. Rogers, *Nature Materials*, 2013, **12**, 938-944.
16. H. Cheng, Y. Zhang, X. Huang, J. A. Rogers and Y. Huang, *Sensors and Actuators A: Physical*, 2013, **203**, 149-153.
17. X. Huang, Y. Liu, H. Cheng, W.-J. Shin, J. A. Fan, Z. Liu, C.-J. Lu, G.-W. Kong, K. Chen, D. Patnaik, S.-H. Lee, S. Hage-Ali, Y. Huang and J. A. Rogers, *Advanced Functional Materials*, 2014, **24**, 3846-3854.
18. T. Sekitani, U. Zschieschang, H. Klauk and T. Someya, *Nature Materials*, 2010, **9**, 1015-1022.
19. T. Sekitani, S. Iba, Y. Kato, Y. Noguchi, T. Someya and T. Sakurai, *Applied Physics Letters*, 2005, **87**, 1-3.
20. M. Kaltenbrunner, T. Sekitani, J. Reeder, T. Yokota, K. Kuribara, T. Tokuhara, M. Drack, R. Schwödiauer, I. Graz, S. Bauer-Gogonea, S. Bauer and T. Someya, *Nature*, 2013, **499**, 458-463.
21. M. Kaltenbrunner, M. S. White, E. D. Głowacki, T. Sekitani, T. Someya, N. S. Sariciftci and S. Bauer, *Nat Commun*, 2012, **3**, 770.
22. D. J. Lipomi, B. C. K. Tee, M. Vosgueritchian and Z. Bao, *Advanced Materials*, 2011, **23**, 1771-1775.
23. M. Vosgueritchian, D. J. Lipomi and Z. Bao, *Advanced Functional Materials*, 2012, **22**, 421-428.
24. D. Khodagholy, J. N. Gelinas, T. Thesen, W. Doyle, O. Devinsky, G. G. Malliaras and G. Buzsaki, *Nat Neurosci*, 2015, **18**, 310-315.
25. F. Greco, A. Zucca, S. Taccola, A. Menciassi, T. Fujie, H. Haniuda, S. Takeoka, P. Dario and V. Mattoli, *Soft Matter*, 2011, **7**, 10642-10650.
26. T. Fujie, Y. Okamura and S. Takeoka, *Advanced Materials*, 2007, **19**, 3549-3553.
27. T. Fujie, N. Matsutani, M. Kinoshita, Y. Okamura, A. Saito and S. Takeoka, *Advanced Functional Materials*, 2009, **19**, 2560-2568.
28. T. Fujie and S. Takeoka, in *Nanobiotechnology*, eds. D. A. Phoenix and A. Waqar, One Central Press, United Kingdom, 2014, pp. 68-94.
29. F. Greco, A. Zucca, S. Taccola, B. Mazzolai and V. Mattoli, *ACS Applied Materials & Interfaces*, 2013, **5**, 9461-9469.

30. S. Taccola, F. Greco, B. Mazzolai, V. Mattoli and E. W. H. Jager, *Journal of Micromechanics and Microengineering*, 2013, **23**.
31. S. Taccola, F. Greco, A. Zucca, C. Innocenti, C. De Julián Fernández, G. Campo, C. Sangregorio, B. Mazzolai and V. Mattoli, *ACS Applied Materials and Interfaces*, 2013, **5**, 6324-6332.
32. A. Zucca, C. Cipriani, S. Sudha, S. Tarantino, D. Ricci, V. Mattoli and F. Greco, *Advanced Healthcare Materials*, 2015.
33. J. Huang, P. F. Miller, J. S. Wilson, A. J. de Mello, J. C. de Mello and D. D. C. Bradley, *Advanced Functional Materials*, 2005, **15**, 290-296.
34. I. Cruz-Cruz, M. Reyes-Reyes, M. A. Aguilar-Frutis, A. G. Rodriguez and R. López-Sandoval, *Synthetic Metals*, 2010, **160**, 1501-1506.
35. A. M. Nardes, R. A. J. Janssen and M. Kemerink, *Advanced Functional Materials*, 2008, **18**, 865-871.
36. W. Fan, T. Kinnunen, A. Niinimäki and M. Hannuksela, *American Journal of Contact Dermatitis*, 1991, **2**, 181-183.
37. S. K. M. Jönsson, J. Birgerson, X. Crispin, G. Greczynski, W. Osikowicz, A. W. Denier van der Gon, W. R. Salaneck and M. Fahlman, *Synthetic Metals*, 2003, **139**, 1-10.
38. D. M. DeLongchamp, B. D. Vogt, C. M. Brooks, K. Kano, J. Obrzut, C. A. Richter, O. A. Kirillov and E. K. Lin, *Langmuir*, 2005, **21**, 11480-11483.
39. S. Baba, T. Midorikawa and T. Nakano, *Applied Surface Science*, 1999, **144–145**, 344-349.
40. Y. Okamura, K. Kabata, M. Kinoshita, D. Saitoh and S. Takeoka, *Advanced Materials*, 2009, **21**, 4388-4392.
41. X. Shi, T. Fujie, A. Saito, S. Takeoka, Y. Hou, Y. Shu, M. Chen, H. Wu and A. Khademhosseini, *Advanced Materials*, 2014, **26**, 3290-3296.
42. T. Fujie, Y. Kawamoto, H. Haniuda, A. Saito, K. Kabata, Y. Honda, E. Ohmori, T. Asahi and S. Takeoka, *Macromolecules*, 2013, **46**, 395-402.
43. F. Herrmann and L. Mandol, *The Journal of Investigative Dermatology*, 1955, **24**, 225-246.
44. T. A. R. Skotheim, John R, ed., *Conjugated Polymers: Processing and Applications*, CRC Press, Boca Raton, 2007.
45. M. M. De Kok, M. Buechel, S. I. E. Vulto, P. Van De Weyer, E. A. Meulenkamp, S. H. P. M. De Winter, A. J. G. Mank, H. J. M. Vorstenbosch, C. H. L. Weijtens and V. Van Elsbergen, *Physica Status Solidi (A) Applied Research*, 2004, **201**, 1342-1359.
46. C. Cipriani, C. Antfolk, M. Controzzi, G. Lundborg, B. Rosen, M. C. Carrozza and F. Sebelius, *Neural Systems and Rehabilitation Engineering, IEEE Transactions on*, 2011, **19**, 260-270.
47. K. Nazarpour, C. Cipriani, D. Farina and T. Kuiken, *Neural Systems and Rehabilitation Engineering, IEEE Transactions on*, 2014, **22**, 711-715.

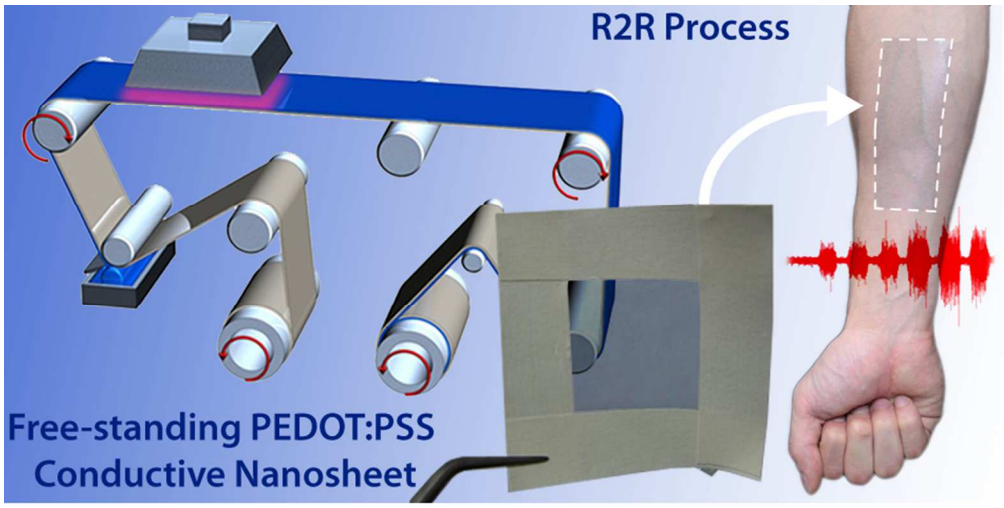

A roll-to-roll process is reported for the preparation of free-standing conductive polymer nanosheets on large areas. Nanosheets are transferred in conformal contact to target surfaces (including skin) and act as unperceivable bio-electrodes.
80x40mm (300 x 300 DPI)